

Pressure-induced lattice instabilities and superconductivity in YBCO

M. Calamiotou¹, A. Gantis¹, E. Siranidi², D. Lampakis², J. Karpinski³, and E. Liarokapis²
¹*Solid State Physics Department, School of Physics, University of Athens, GR-15784 Athens, Greece*
²*Department of Physics, National Technical University of Athens, 157 80 Athens, Greece and*
³*Laboratory for Solid State Physics, ETH, CH-8093 Zürich, Switzerland*

Combined synchrotron angle-dispersive powder diffraction and micro-Raman spectroscopy are used to investigate pressure-induced lattice instabilities that are accompanied by superconducting T_c anomalies in $\text{YBa}_2\text{Cu}_4\text{O}_8$ and optimally doped $\text{YBa}_2\text{Cu}_3\text{O}_{7-\delta}$, in comparison with the non-superconducting $\text{PrBa}_2\text{Cu}_3\text{O}_{6.92}$. In the first two superconducting systems there is a clear anomaly and hysteresis in the evolution of the lattice parameters and increasing lattice disorder with pressure, which starts at ≈ 3.7 GPa. On the contrary, in the Pr-compound the lattice parameters follow very well the expected equation of state (EOS) up to 7 GPa. The micro-Raman data of the superconducting compounds show that the energy and width of the A_g phonons exhibit anomalies over the same pressure range where the lattice parameters deviate from the EOS and the average $\text{Cu}_2\text{-O}_{pl}$ bond length exhibits a strong contraction that correlates with the non-linear pressure dependence of T_c . The anomalous Raman behavior is not observed for the non superconducting Pr compound, clearly indicating a connection with the charge carriers. It appears that the cuprates close to optimal doping are at the edge of lattice instability.

PACS numbers: 61.05.cp, 74.25.Kc, 74.72.-h, 64.75.-g

Introduction

It is well accepted that structural and electronic inhomogeneities constitute intrinsic properties of cuprate superconductors [1–3]. To this context the study of any lattice distortions induced by application of either internal chemical or external hydrostatic pressure [4–6] that modify the transition temperature (T_c) is important for understanding the role of lattice effects in the high T_c superconductivity. Lattice instabilities in hydrostatically compressed $\text{YBa}_2\text{Cu}_3\text{O}_y$ (Y123) and $\text{YBa}_2\text{Cu}_4\text{O}_8$ (Y124) cuprates where T_c dependence on pressure shows saturation or non-linear behavior [7, 8], manifest themselves in the Raman phonon frequencies as a deviation from an expected linear behavior at a critical pressure range 2.5-6 GPa [9, 10]. Recent structural investigations, using synchrotron angle-dispersive powder diffraction and dense sampling on optimally doped Y123 superconductor, have revealed in the pressure range $3.7 \text{ GPa} < p < 10 \text{ GPa}$ a clear deviation of the lattice constants from the expected EOS, strong hysteresis effects, and the formation of an additional new textured phase [6]. Interatomic distances in the unit cell of Y123 such as the Ba distance from the basal plane, the $\text{Cu}_2\text{-O}_{pl}$ bond length, and the $\text{Cu}_2\text{-Cu}_1$ distance along the c -axis have been found to exhibit also a non linear evolution with applied pressure that correlates with modifications of the Raman spectra of the in-phase O_{pl} and the O_{ap} phonon modes [6]. The correlation of the structural characteristics with the Raman frequency modifications [6] and corresponding changes of T_c [7] imply that the trigger of the lattice instabilities lies among the CuO_2 and BaO planes. Charge redistribution among the planes, that has been found to occur in the case of chemical pressure [11], also affects the T_c , and must certainly play a role in the observed effects.

The main questions that arise is whether similar effects

are present in other cuprates and how they relate to the amount of charge carriers and superconductivity. The isostructural to Y123 compound $\text{PrBa}_2\text{Cu}_3\text{O}_7$ (Pr123) is a good example to study, having apparently no free carriers [5]. Structural and Raman studies under hydrostatic pressure in this compound are absent. The Y124 superconductor is another good case study, since it can be considered as a model compound for the underdoped region of the YBCO system. Previous structural studies under hydrostatic pressure up to 5 GPa (using a laboratory source) gave only some marginal evidence of a non-linear pressure dependence above 4 GPa [12]. We present here high quality synchrotron angle-dispersive powder diffraction data and micro-Raman spectra under hydrostatic pressure for the Pr123 ($T_c=0\text{K}$) and Y124 ($T_c=80\text{K}$) compounds in comparison with the corresponding ones for Y123 ($T_c=92\text{K}$) [6]. The pressure region up to 13 GPa has been investigated with a pressure step of ≈ 0.5 GPa. Our combined structural and spectroscopic results provide strong evidence that the presence of charge carriers and the pressure-induced lattice instabilities in the superconducting cuprates are strongly related, thus affecting the T_c dependence on pressure.

Experimental details

We have studied a powder $\text{PrBa}_2\text{Cu}_3\text{O}_{6.92}$ sample with an oxygen content comparable to the previously investigated optimally doped Y123 [6] and the $\text{YBa}_2\text{Cu}_4\text{O}_8$ compounds. Synchrotron angle-dispersive powder diffraction experiments at high pressures have been carried out at the Swiss-Norwegian beamline BM01A of ESRF (Grenoble), using a diamond anvil cell (DAC) and a 4:1 methanol-ethanol mixture as pressure medium, which is known to remain hydrostatic and do

not cause peak broadening in powder samples at least up to ~ 10 GPa [13]. Ruby crystals were used for measuring the pressure and monitoring any inhomogeneity in the pressure distribution. Diffraction patterns have been collected with a wavelength $\lambda=0.7117\text{\AA}$ and a MAR345 image plate detector. The pressure cell was left to relax for approx. 20-30 min at each pressure. The 2D raw images have been converted to 2θ patterns, after correcting for distortions and refining the detector-sample distance using a LaB₆ standard by the program FIT-2D [14].

The Raman spectra were obtained at room temperature and high hydrostatic pressures with a T64000 JobinYvon triple spectrometer equipped with a liquid nitrogen cooled charge coupled device (CCD) and a microscope lens of magnification $\times 40$. A Merrill Bassett type diamond anvil cell (DAC) was used for the high-pressure measurements (up to 6.8 GPa), which allowed the Raman studies to be carried out in a back scattering geometry. The pressure-transmitting medium was a mixture of methanol-ethanol, with analogy (4:1). Silicon single crystals distributed around the sample were used for calibration of the pressure and for monitoring the hydrostatic conditions. The 514.5 nm line from an Ar⁺ laser was used for excitation, which produced the lowest luminescence from the diamonds. The laser beam was focused on the sample at a spot of diameter 4 μm while the power level was kept below 0.20 mW. Typical accumulation times were up to 3 hours depending on the scattering polarization.

Results

A. Average structure

Structural data have been obtained by analyzing the intensity-vs- 2θ diffraction patterns with the Rietveld method using Fullprof [15] and a pseudo-Voigt line profile function. The diffraction patterns of Pr123 have been refined with the orthorhombic Pmmm space group in the whole pressure region. Minor impurity lines belonging to BaCuO₂ [5] have been excluded. Lattice constants for Y124 have been refined with the Ammm space group using the LeBail method, implemented in Fullprof [15]. Weak peaks appearing for $p \geq 3.7\text{GPa}$ have been excluded as discussed below. Fig.1a shows a characteristic synchrotron diffraction pattern of Pr123, at $p = 4.7$ GPa, together with the results of the Rietveld refinement and Fig.1b the corresponding pattern of Y124 with the results of LeBail refinement. The pressure dependence of the a-, b-axis is shown in Fig.2a for Pr123, Fig.2b for Y123 (from ref.[6]), and Fig.2c for Y124. The evolution of the c-axis with the applied hydrostatic pressure for Pr123 is shown in Fig.3a in comparison with the corresponding one for the optimally doped Y123 (Fig.3b) from ref.[6], whereas the results for Y124 are presented in Fig.3c. Full symbols represent the values for increasing the pressure and open symbols those for releasing the

pressure. In the case of Y124, we have also carried out measurements while increasing again the pressure after pressure release (full triangles in Fig.2c and Figs.3c, 3f). The lattice constants have been fitted to the empirical Murnaghan equation of state $q = q_0[p(\kappa_q/\kappa'_q) + 1]^{-\kappa'_q}$, where p is the applied pressure, q is the lattice constant under compression, κ_q its compressibility and κ'_q a parameter that expresses the pressure dependence of the compressibility. For Pr123 the solid lines are fits to the data for increasing pressure up to 7 GPa. For Y123 and Y124 the solid lines are fits to the data for increasing pressure where the pressure region $3.7 < p < 8$ GPa has been excluded as it will be discussed below. The values of $\kappa_a = 2.6 \times 10^{-3} \text{GPa}^{-1}$, $\kappa_b = 2.1 \times 10^{-3} \text{GPa}^{-1}$ and $\kappa_c = 4.1 \times 10^{-3} \text{GPa}^{-1}$ obtained for Pr123 are slightly smaller but comparable to those of Y123 [6]. The Y124 compound exhibits strong anisotropy in all three lattice directions with corresponding compressibilities $\kappa_a = 3.7 \times 10^{-3} \text{GPa}^{-1}$, $\kappa_b = 1.9 \times 10^{-3} \text{GPa}^{-1}$ and $\kappa_c = 4.5 \times 10^{-3} \text{GPa}^{-1}$. Upon decompression the c axis evolution of the Y124 compound can be best described by the dashed line (Fig.3c), which is a Murnaghan equation with $\kappa_c = 4.2 \times 10^{-3} \text{GPa}^{-1}$ and a much bigger κ'_c value compared to the corresponding one for pressure increase.

For Pr123 the evolution of all lattice constants with increasing pressure follows very well the Murnaghan equation of state up to ~ 7 GPa. Upon pressure release the effect of pressure on the unit cell is reversible, i.e. the values of lattice constants coincide with those at increasing pressure. This is in contrast with the evolution of the c-axis of the Y123 compound. The c-axis exhibits a strong deviation from the expected equation of state that starts around 3.7 GPa and extends to 8-10 GPa, and there is a clear irreversibility of the effect of pressure, which results in a strong hysteresis [6]. The c-axis of Y124 shows also a deviation from EOS in the same pressure region, however the effect is less intense than in Y123.

The a- and b-axis of Y123 deviate also from the EOS [6], but to a smaller degree than the c-axis (Fig.2b). For Pr123 no deviation is detected (Fig.2a), while for Y124 the deviation in the b- and a-axis is more pronounced than in Y123, with the b-axis showing a larger deviation than the a-axis (Fig.2c). It is worth to mention that when pressure was increased again in Y124 after pressure release, the values of the c-axis are placed between the data of pressure increase and pressure release, but closer to the second data (Fig.3c). In the case of the a- and b-axis, the increase of pressure for a second time brings the data closer to those of pressure release for the a-axis and of the original pressure increase for the b-axis. However, the observed modifications in those axes are much smaller than for c-axis and the effect might be related to the anisotropy of the compound. For Pr123 and Y123 we have no data with increasing pressure for a second time to compare, but as for Pr123 there is no deviation from the EOS and the data of pressure increase or release coincide, we could not observe any changes. Furthermore, in Y123 the deviations from the EOS for the a- and b-axis are

smaller than in Y124 and any changes, even if present, might not be able to be detected.

B. Microstructure

With increasing pressure the width of the diffraction peaks is increasing. In the case of Y123, the Williamson-Hall plots have revealed that the application of pressure induces a microstrain-type diffraction peak broadening while size-type broadening is negligibly small [6]. Although it is very difficult to assess the origin of microstrains, pressure-induced disorder is most likely associated with the observed line broadening in the pressure region up to 10 GPa. In order to examine any correlation of pressure-induced disorder to the observed deviations from the expected EOS, we have estimated the upper limit of apparent microstrains-disorder in all compounds. Since we are interested to investigate their evolution with pressure rather than absolute values, we have used the width of the single, non overlapping 113 Bragg peak. The width of the 113 reflection is not affected by intrinsic defects, such as dislocations and stacking faults, as we have found in the case of Pr123 [5]. The 113 peaks have been fitted with a pseudo-Voigt function and the apparent microstrain, ε , has been calculated as $\varepsilon = (W - W_i)/\tan\theta$, where W and W_i are the full widths at half maximum of the sample and the standard LaB₆ respectively, that has been used to determine the instrumental resolution.

The evolution of microstrains-disorder with pressure for Pr123, Y123 and Y124 is shown in Fig.3d, 3e and 3f respectively. Full symbols correspond to the values for increasing the pressure and open symbols to those for releasing the pressure. Dotted lines are guide to the eye to emphasize the regions with different increase of disorder upon pressure. Fig.3d shows that microstrains in Pr123 remain almost constant up to a pressure of 7 GPa, starting to increase exactly at the same pressure where the c-axis deviates from the expected equation of state. *No irreversibility and hysteresis effects are observed.* On the contrary, the microstrains of Y123 start to increase at $p \sim 3.7$ GPa where the c-axis deviates from the equation of state, for $p > 7$ GPa they continue to increase with a bigger slope and for $p > 10$ GPa they increase further. In addition *pronounced hysteresis effects are present* (Fig.3e). Analogous results have been obtained for Y124 (Fig.3f). It is clear from Fig.3 that the increase of microstrains occurs in all cases exactly at the same pressure where there is an anomaly in the expected lattice constants behavior on pressure. With the reduction of pressure to ambient conditions, the Pr123 compound practically returns to the original state of microstrains indicating that they are not permanent lattice distortions. On the contrary, the Y123 and Y124 compounds show hysteresis in the whole pressure range. It should be noted that, the 2D patterns obtained with the *cake* function of the FIT2D [14] software do not bear any sign of a non-hydrostatic pressure on the diffraction lines of Pr123, Y123 (Fig.4 in ref.[6])

and Y124. This is in agreement with all measurements performed up to now that do not provide any evidence for a non hydrostatic environment in the methanol-ethanol mixture for pressures up to 10 GPa.

C. Raman spectra

Typical Raman spectra of the hydrostatically compressed Pr123 compound are shown in Fig.4. All five A_g symmetry phonons with eigenvectors along the c-axis were studied in the two scattering polarizations, xx (Fig.4a) and zz (Fig.4b) corresponding to incident and scattered light polarization parallel or perpendicular to the CuO₂ planes. Those are at ~ 128 cm⁻¹ (Ba-atom), ~ 150 cm⁻¹ (Cu_{p1}-atom), ~ 300 cm⁻¹ (out of phase (B_{1g}-like) vibrations of the O_{p1} atoms), ~ 435 cm⁻¹ (in phase vibrations of the O_{p1} atoms) and ~ 523 cm⁻¹ (vibrations of the O_{ap} atoms). Fig.5 shows that the energy of the four A_g symmetry phonons in Pr123 increases almost linearly with pressure. For comparison, the pressure dependence of the ortho-I and ortho-II phases of Y123, corresponding to oxygen content ≈ 7 (Y123) and ≈ 6.5 (Y1236.5), are also shown, where it is clear that in the region 2.5-4 GPa there is no increase in the phonon energy despite the increase in pressure. *This softening of the four A_g phonons is in contrast to their almost linear behavior for Pr123.* For the B_{1g}-like mode the phonon energy has been found to increase almost linearly with increasing pressure, as expected, without showing any anomaly, for all compounds.

Figure 6 presents the variation of the corresponding phonon width of the four A_g symmetry phonons for the sets of compounds, which again indicates that both Y123 and Y1236.5 have an unusual behavior with pressure compared with Pr123. Especially the apical phonon mode shows a considerable increase in width for $p \approx 2$ GPa and then a decrease to almost the original value for $p \approx 3.7$ GPa followed by an increase. This unconventional variation of the width with pressure is not a result of error in the fitting procedure, as it is quite clear from the spectra (Fig.1 of ref. [9]). The initial increase in width and frequency of the mode up to ≈ 2 GPa is a typical increase of the modes with pressure. Afterwards, both the width and the frequency show abnormal behavior, which indicates that another mechanism is active. This could be a pressure induced lattice instability that results in phase separation, mode frequency softening, and decrease in the width, which finally relaxes the internal strains.

Discussion

The evolution of microstrains-disorder in Pr123 indicates two regions of almost linear pressure dependence for the compound; namely for pressures up to 7 GPa and above that (Fig.3d). The increase of disorder for $7 < p \leq 10$ GPa which correlates with the deviation of the

c-axis values from the expected EOS (Fig.3a) would imply that the system undergoes a phase transition likely related to a distorted orthorhombic phase. In the case of Y123 and Y124 additional features are evident in the microstrains-disorder evolution on pressure. There is an intermediate pressure region (3.7-7 GPa), where microstrains exhibit again an almost linear increase on pressure but with a different slope (Fig.3e and 3f). Interestingly, in the two pressure regions, i.e., $p < 3.7\text{GPa}$ and $7 < p \leq 10\text{GPa}$ microstrains increase with the same pressure slopes in the Pr123, Y123 and Y124 compounds. Since Pr123 and Y123 have the same structure and comparable compressibilities, the increased microstrains-disorder in the intermediate (3.7-7 GPa) pressure region (observed under the same experimental conditions only in Y123 and Y124) implies that pressure-induced disorder in that region is an intrinsic effect of Y123 and Y124. It should be mentioned that at the pressure of $\approx 3.7\text{GPa}$ four new weak Bragg peaks appear in the diffraction patterns of both Y123 (Fig.3 in ref.[6]) and Y124 (Fig.1b), which are not observed in Pr123 (Fig.1a). The new weak lines could not be due to the formation of a superstructure, as the systematic investigation of all observed lines has proved. Moreover the 2D diffraction images revealed that these new lines exhibit strong texture and strain effects unlikely to those of the main phase (Fig.4 in ref.[6]). We therefore assume that they are due to the formation of an additional textured and distorted phase at this critical pressure in both Y123 and Y124 compounds. The new weak lines disappear completely upon pressure release below roughly the same pressure ($\approx 3\text{GPa}$) (Fig.3 in ref.[6]). When pressure is increased again in Y124 after pressure release they appear again however their intensity is strongly reduced implying a correlation of the presence of the new phase with the corresponding c-axis anomaly (Fig.3c).

The increased disorder in both Y124 and Y123 compounds over the intermediate (3.7-7 GPa) pressure region appears together with the hysteresis, the anomaly in the lattice constants evolution (Fig.3) and the new lines reminiscent of the development of a new phase. In the diffraction pattern of Y124, we have also observed at 10.3 GPa the appearance of two additional lines at $2\theta \approx 15.5$ and 28 degrees, with texture effects, which disappear again for $p < 9\text{GPa}$ on decompression. At the same pressure the b-axis deviates from the expected equation of state. The formation of the new phases happens at the pressure where there is a deviation from the EOS, and whenever this does not occur, as in Pr123, the new lines do not appear. Apparently, they are related with a phase separation, which is triggered by the hydrostatic pressure and causes deviations from the EOS. To this context the different microstrain regions marked by dotted straight lines with a different pressure slope in Figures 3(e) and 3(f) may indicate the formation of different distorted orthorhombic micro-phases in Y123 and Y124. All these effects are absent in Pr123 up to a pressure of 7 GPa.

For the in-phase mode the high-pressure Raman re-

sults for the Y123 compound have indicated modifications, which appear as a double peak at about 2 GPa [16], i.e. at the pressure where the bond distance Cu2-O_{pl} and the position of the Ba atom show a non-linear dependence on pressure [6]. Similar modifications from linearity with increasing pressure were also detected for the apical oxygen frequency [16], which correlates (as expected) with the pressure dependence of the Cu2-Cu1 bond lengths [6]. The same Raman results have also been obtained for the Y124 compound [10, 16]. However, the non superconducting Pr123 compound does not show such anomalies. In complete agreement with the corresponding Raman results, the average Cu2-O_{pl} bond length obtained from the Rietveld refinement for Pr123 (shown in Fig.7a) exhibits only a very small, if any, modification at the characteristic pressure of $\approx 3.7\text{GPa}$ contrary to the results of the Y123 compound (Fig.7b). The abrupt contraction of the Cu2-O_{pl} bond in Y123 at $\approx 3.7\text{GPa}$ may be related to a *pressure-induced charge redistribution*.

The combined XRD and Raman results show for Y123 and Y124 in the pressure region $3.7 < p < 8\text{GPa}$; a clear deviation from the expected EOS of the c-axis (Figs.3b, 3c), modifications of disorder (Figs.3e, 3f), which correlate with a softening of the four A_g phonons (Fig.5) and anomaly in their width (Fig.6). Furthermore, there is also a strong irreversibility and hysteresis together with the appearance of a new phase. In the corresponding data of the isostructural Pr123 no similar phenomena are observed. One could assume that for $3.7 < p < 8\text{GPa}$ a new phase is created with pressure in these cuprates, which is accompanied by modifications in the lattice along the Cu2-O_{pl} and Cu2-O_{ap} bonds, directly affecting the electronic states, the carrier distribution, and the transition temperature in Y123 and Y124, while having no appreciable difference in Pr123, which apparently does not have carriers [5]. The main effects are observed for the A_g symmetry phonons with eigenvectors along the c-axis while the B_{1g} phonons are not affected. The pressure data in the cuprates studied point to a lattice instability close to optimal doping, which once exceeded by pressure (present work) or doping [17], induces local lattice distortions mostly in the CuO_2 planes that modify the transition temperature.

Previous studies in both Y123 and Y124 compounds have revealed that at those critical pressures (3.7 GPa and 10.3 GPa) there are modifications of the critical temperature T_c dependence on pressure [7, 8]. Moreover irreversibility and hysteresis were observed in the pressure dependence of T_c for the Y124 compound by Scholtz et al [8]. It was suggested that a possible transformation of the sample for pressures above 20 GPa was the reason for this unexpected hysteresis. However, our data and more precisely the modification of the c-axis compressibility of Y123 and Y124 in the intermediate (3.7-7 GPa) pressure region, which correlates with the increase of microstrains, the appearance of extra Bragg peaks, and the modifications in T_c implies that the origin of these phenomena must be an intrinsic instability of the superconducting

cuprates, which appears at much lower hydrostatic pressures (~ 3.7 GPa), affects T_c and results in the development of another phase that appears together with the deviation from the normal EOS. Such effects and a new phase are absent in the non-superconducting Pr123 at least up to 7 GPa.

Conclusions

Combined synchrotron xrd and Raman measurements from superconducting compounds Y123 and Y124 show pressure-induced lattice anomalies (deviation from the normal EOS of the lattice constants), irreversibility and hysteresis, disorder (estimated by the line broadening), the appearance of additional diffraction peaks apparently related with a new phase, softening and abnormal pressure-dependence of the width for all A_g -symmetry phonon modes. These modifications fully correlate with anomalies in the T_c -dependence on pressure. The absence of similar effects in the non-superconducting isostructural Pr123 is a strong indication that the observed effects are related also with the presence of free carriers. The anomalies in the Raman-active phonon

modes at the same pressures with the bond length changes calculated from the synchrotron diffraction data point to a charge redistribution within and around the CuO_2 planes. This justifies the full correlation with the pressure modifications in the transition temperature and the absence of similar effects in Pr123. Furthermore, it provides a clue that close to optimal doping the cuprates are at a lattice instability, which seems to be an intrinsic property in the compounds studied. Although we cannot anticipate the behavior of the rest of the cuprates, our up-to-now data provide a hint about the role of the lattice in the high T_c superconductivity of the cuprates.

Acknowledgements

We thank the Swiss-Norwegian committee for beam time allocation at the SNBL BM01A, at ESRF, and Prof. V. Dmitriev for discussion and help during the experiments at BM01A. The team from NTUA acknowledges support from CoMePhS (STRP project of E.U.). Partial support from the Research Account of the University of Athens (Kapodistrias) is acknowledged.

-
- [1] E. Dagotto, *Science* **309**, 257 (2005).
 - [2] J. Orenstein, and A. J. Millis, *Science* **288**, 468 (2000).
 - [3] D. Lampakis, E. Liarokapis, and C. Panagopoulos, *Phys. Rev. B* **73**, 174518 (2006).
 - [4] A. Gantis, M. Calamiotou, D. Palles, D. Lampakis, and E. Liarokapis, *Phys. Rev. B* **68**, 064502 (2003).
 - [5] M. Calamiotou, A. Gantis, I. Margiolaki, D. Palles, E. Siranidi, and E. Liarokapis, *J. Phys.: Condens. Matter* **20**, 395224 (2008).
 - [6] M. Calamiotou, A. Gantis, D. Lampakis, E. Siranidi, E. Liarokapis, I. Margiolaki, and K. Conder, *EPL* **85**, 26004 (2009).
 - [7] U. Koch, N. Lotter, J. Wittig, W. Assmus, B. Gegenheimer, and K. Winzer, *Sol. State Comm.* **67**, 959 (1988).
 - [8] J. J. Scholtz, E. N. van Eenige, R. J. Wijngaarden, and R. Griessen, *Phys. Rev. B* **45**, 3077 (1992).
 - [9] E. Liarokapis, D. Lampakis, T. Nishizaki, and C. Panagopoulos, *High Pressure Research* **18**, 109 (2000).
 - [10] D. Lampakis, D. Palles, E. Liarokapis, S. M. Kazakov, and J. Karpinski, *Phys. Rev. B* **72**, 014539 (2005).
 - [11] J. Karpinski, S. M. Kazakov, M. Angst, A. Mironov, M. Mali, and J. Roos, *Phys. Rev. B* **64**, 094518 (2001).
 - [12] R. J. Nelmes, J. S. Loveday, E. Kaldis, and J. Karpinski, *Physica C*, **172** 311 (1990).
 - [13] T. Kenichi, *J. Appl. Phys.*, **89** 662 (2001).
 - [14] A. P. Hammersley, S. O. Svensson, M. Hanfland, A. N. Fitch, and D. Hausermann, *High Press. Res.*, **14** 235 (1996).
 - [15] J. Rodriguez-Carvajal, *Physica B*, **192** 55 (1993).
 - [16] D. Lampakis, E. Liarokapis, J. Karpinski, C. Panagopoulos, and T. Nishizaki, *Journal of Superconductivity: Incorporating Novel Magnetism*, **17**, 121 (2004).
 - [17] E. Kaldis, J. Rohler, E. Liarokapis, N. Poulakis, K. Con-

der, and P.W. Loeffen, *Phys. Rev. Lett.* **79**, 4894 (1997).

FIGURE CAPTIONS

Figure 1. (Color online) Rietveld refinement of synchrotron powder diffraction patterns for Pr123 at $p=4.7$ GPa (a) and LeBail refinement for Y124 at $p=4.7$ GPa (b). Experimental (circles), calculated (continuous line) intensities, their difference (bottom line) and corresponding positions of Bragg peaks (bars). The part of the pattern near $2\theta=20^\circ$, where the lines from the gasket appear, has been excluded. (*) shows the peaks of impurity BaCuO_2 in Pr123 and (\diamond) the weak peaks appearing for $p \geq 3.7 \text{ GPa}$ in Y124.

Figure 2. (Color online) Pressure dependence of the a -, b -axis for the Pr123 (a), Y123 (ref. [6]) (b) and Y124 (c) compounds. Full symbols correspond to increasing pressure and open symbols to pressure release. Full triangles correspond to the increase of pressure for second time. Solid lines are fits to the Murnaghan EOS.

Figure 3. (Color online) Pressure dependence of the c -axis for the Pr123 (a), Y123 (from ref. [6]) (b) and Y124 (c) compounds. Evolution of apparent disorder ε with applied pressure for the Pr123 (d), Y123 (e) and Y124 (f) compounds. Full symbols correspond to increasing pressure and open symbols to pressure release. Full triangles correspond to the increase of pressure for second

time. Solid lines (and dashed line in 2c) are fits to the Murnaghan EOS as described in the text. Dotted lines in 2d-f are guide to the eye to emphasize the regions with different increase of disorder upon pressure.

Figure 4. Typical Raman spectra of the Pr123 compound at selected pressures in the xx (a) and zz (b) scattering configuration.

Figure 5. (Color online) The variation of the energy of the Cu_{pl} (a), O_{ap} (b), Ba (c) and O_{pl} (d) phonon upon pressure for different cuprates; $\text{YBa}_2\text{Cu}_3\text{O}_{6.5}$ (Y1236.5),

$\text{YBa}_2\text{Cu}_3\text{O}_7$ (Y123) and Pr123.

Figure 6. (Color online) The variation of the width of the Cu_{pl} (a), O_{ap} (b), Ba (c) and O_{pl} (d) phonon upon pressure for the cuprates of Fig.5.

Figure 7. The pressure dependence of the Cu2- O_{pl} bond length for the Pr123 (a) in comparison to that of Y123 (ref. [6])(b). Dashed lines are guide to the eye.

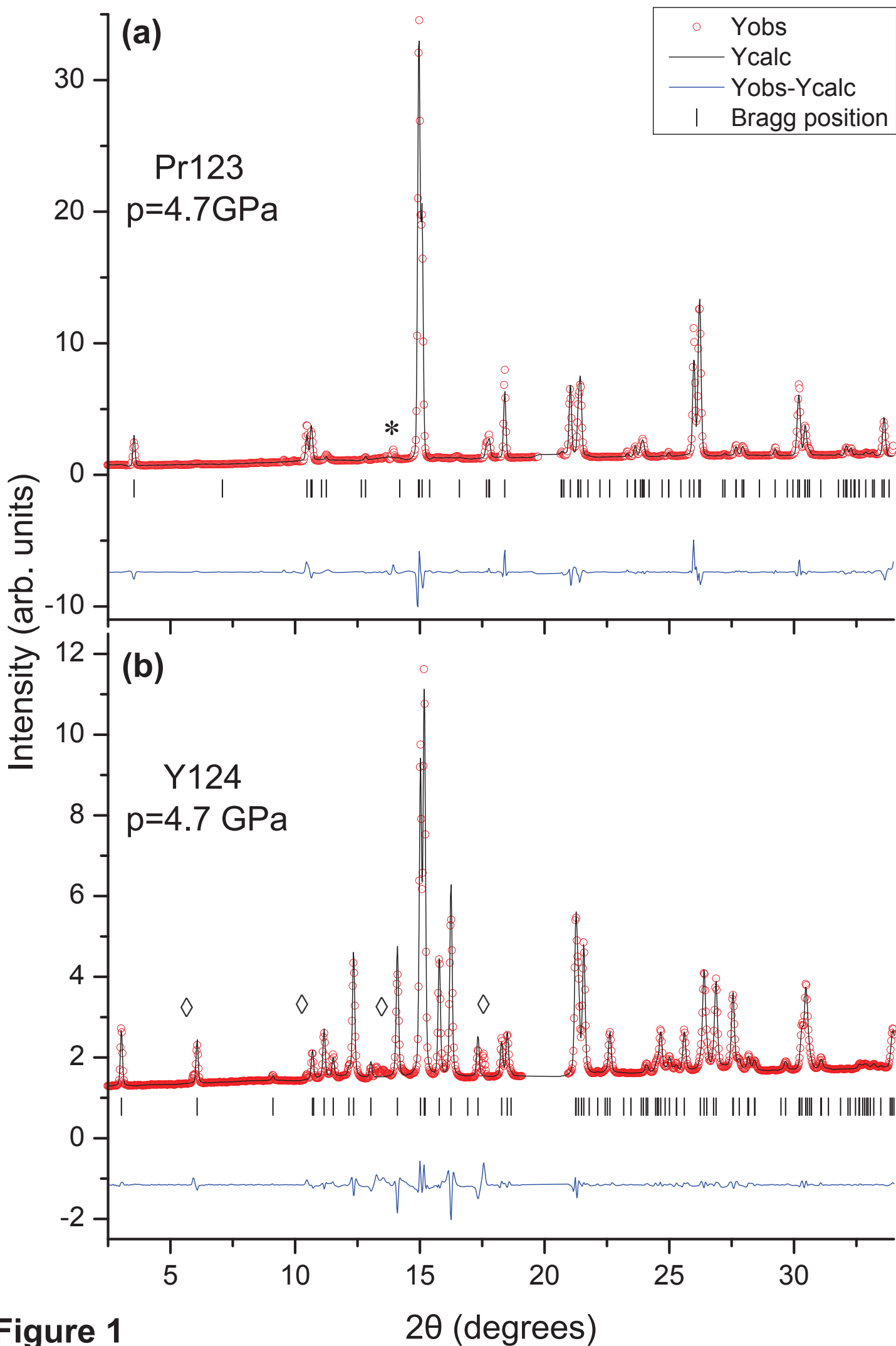


Figure 1

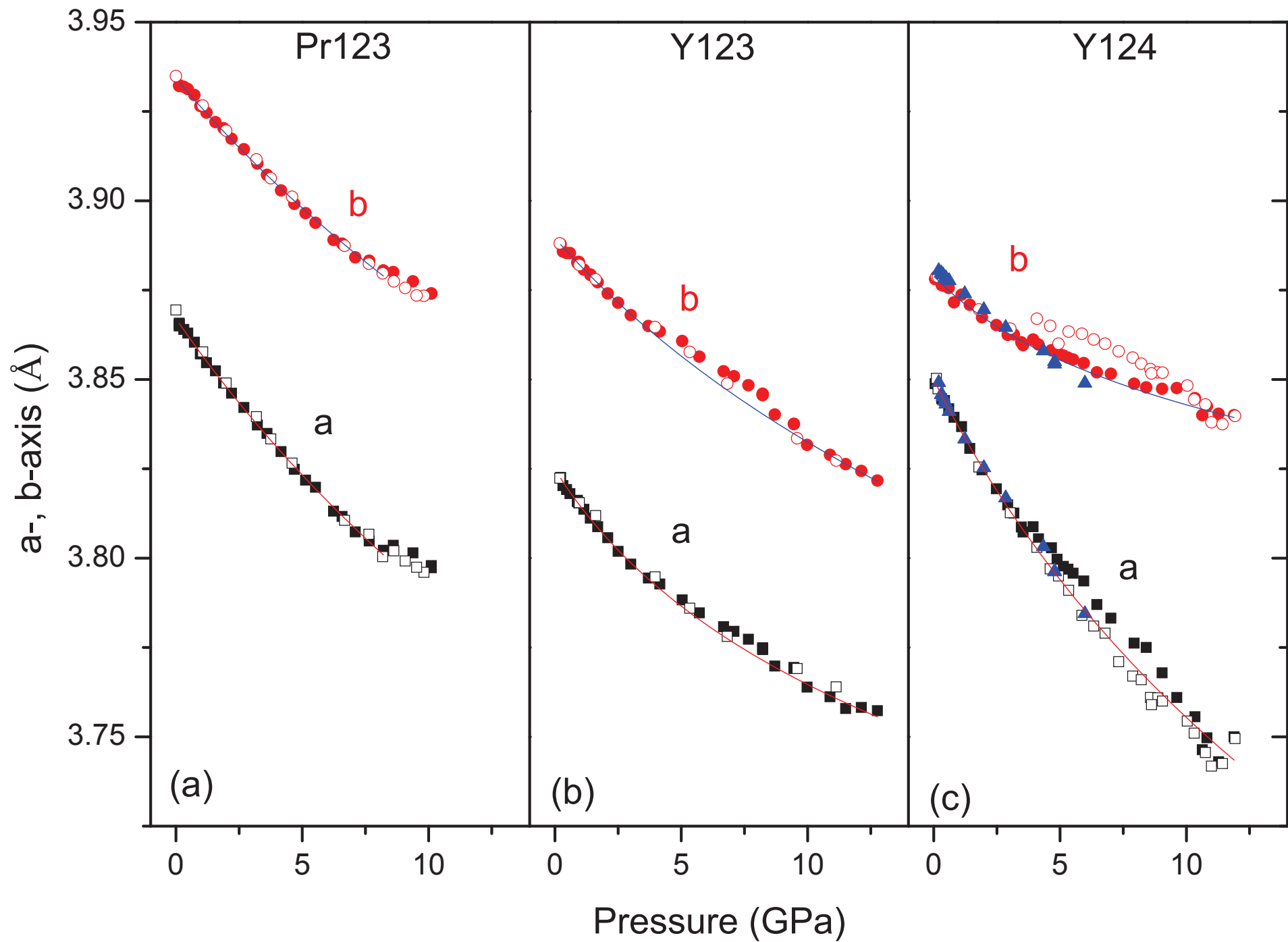


Figure 2

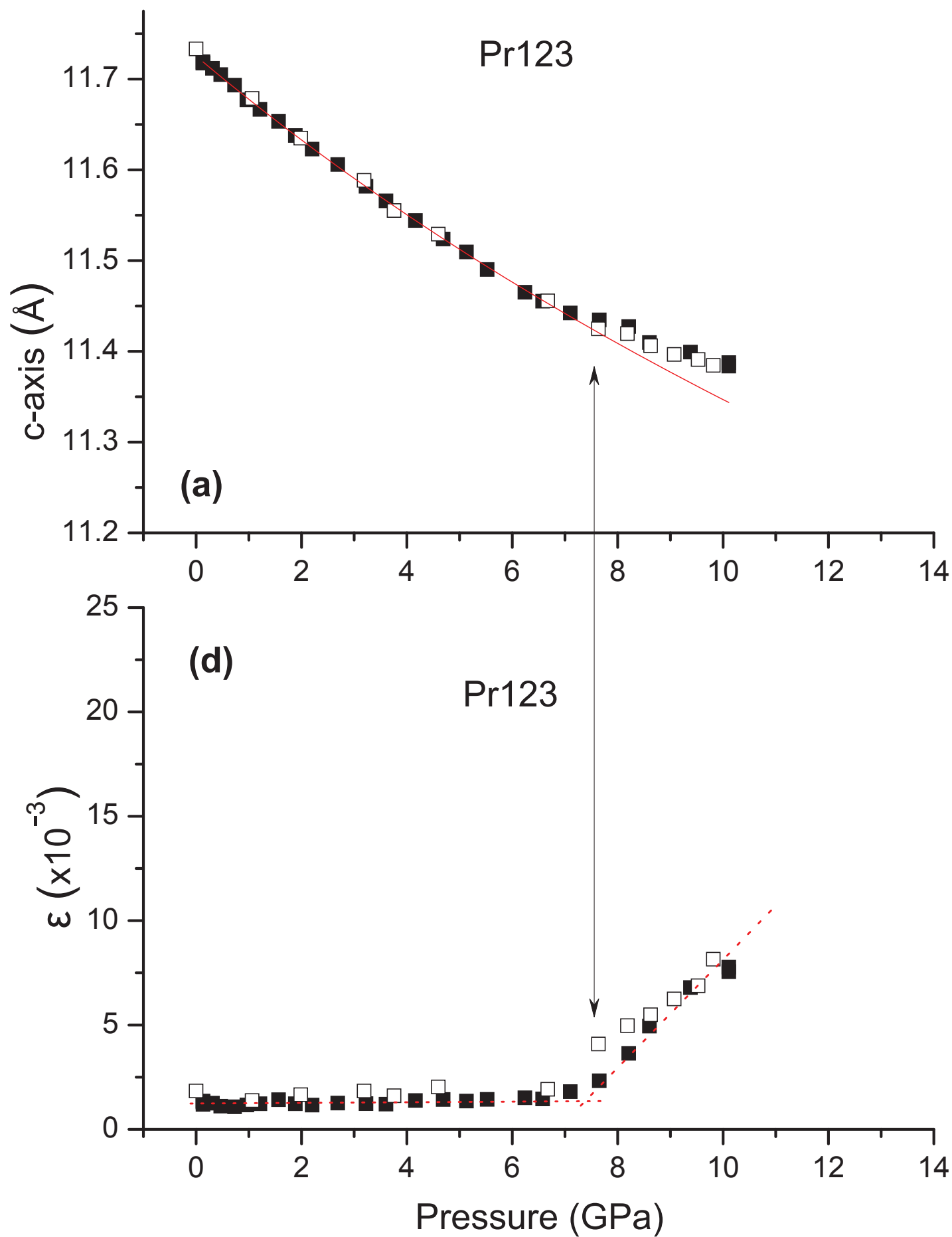


Figure 3a_d

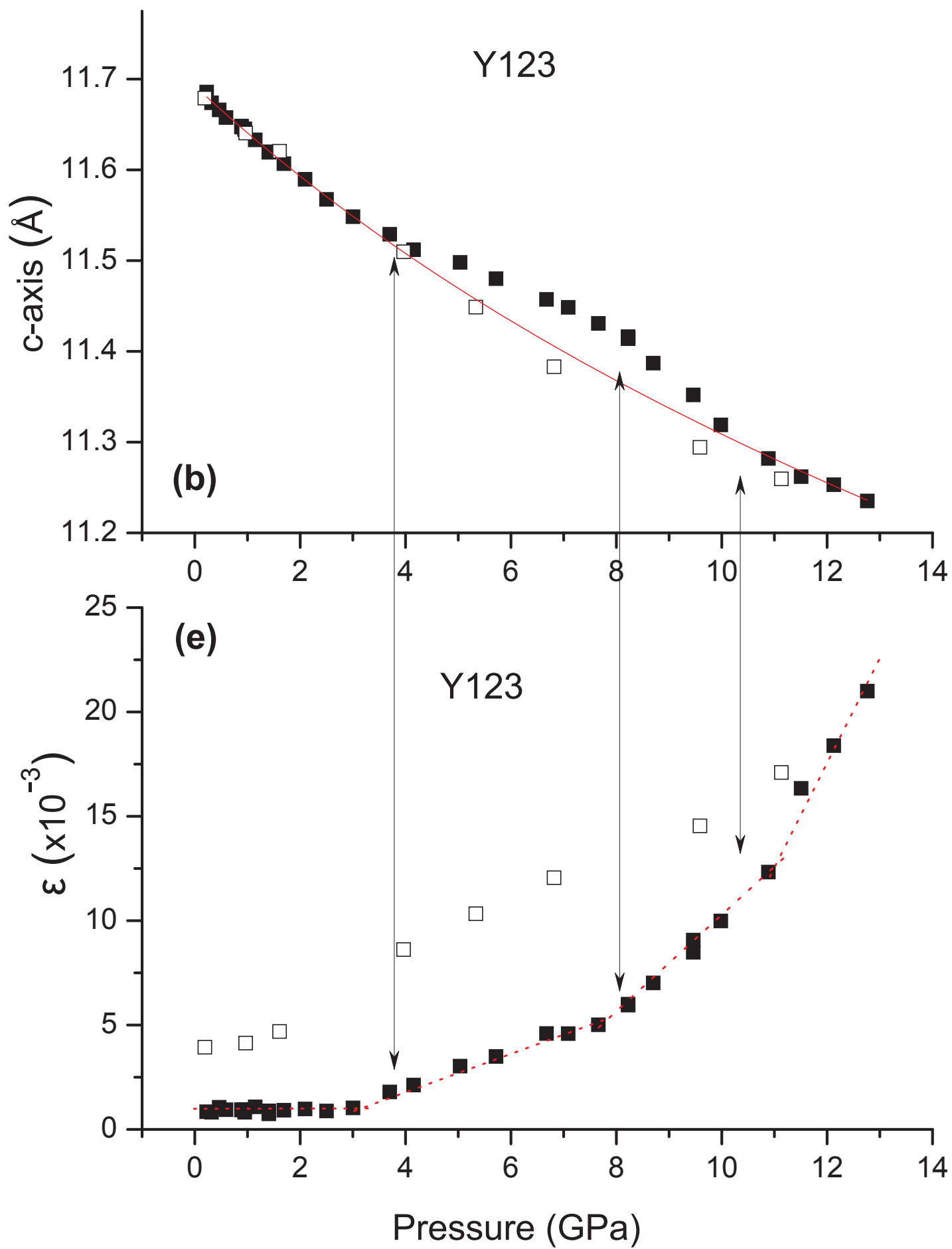


Figure 3b_e

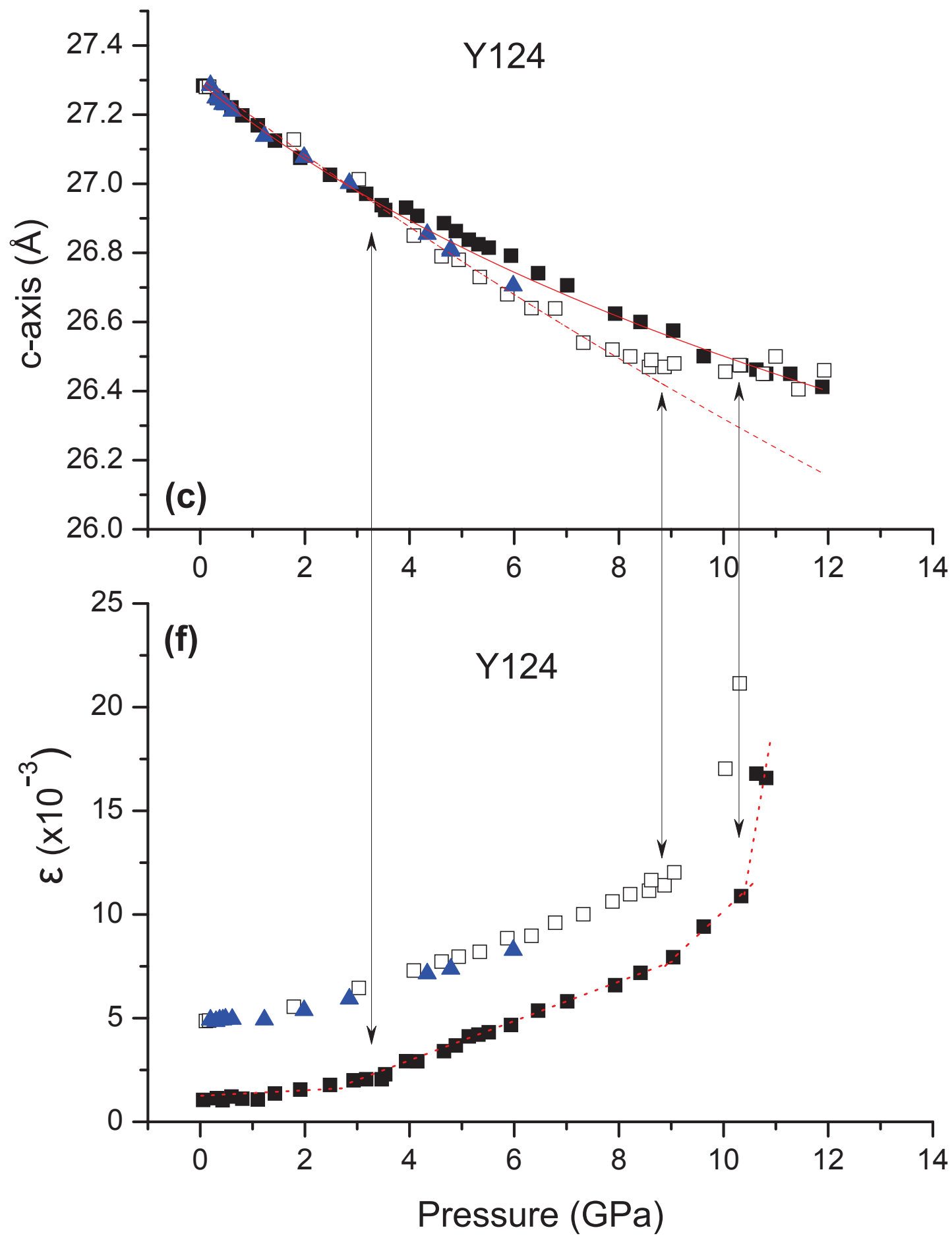


Figure 3c_f

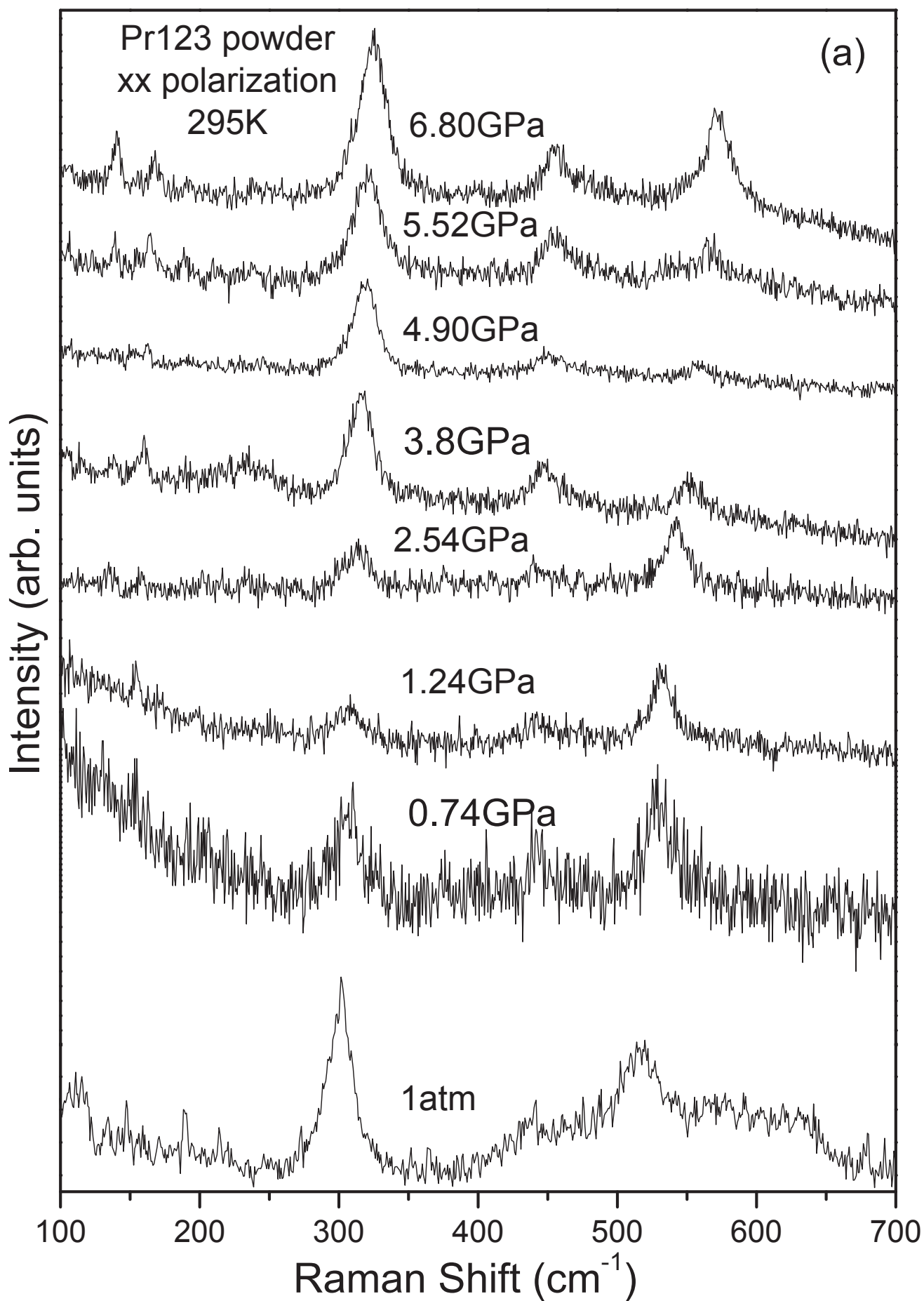


Figure 4a

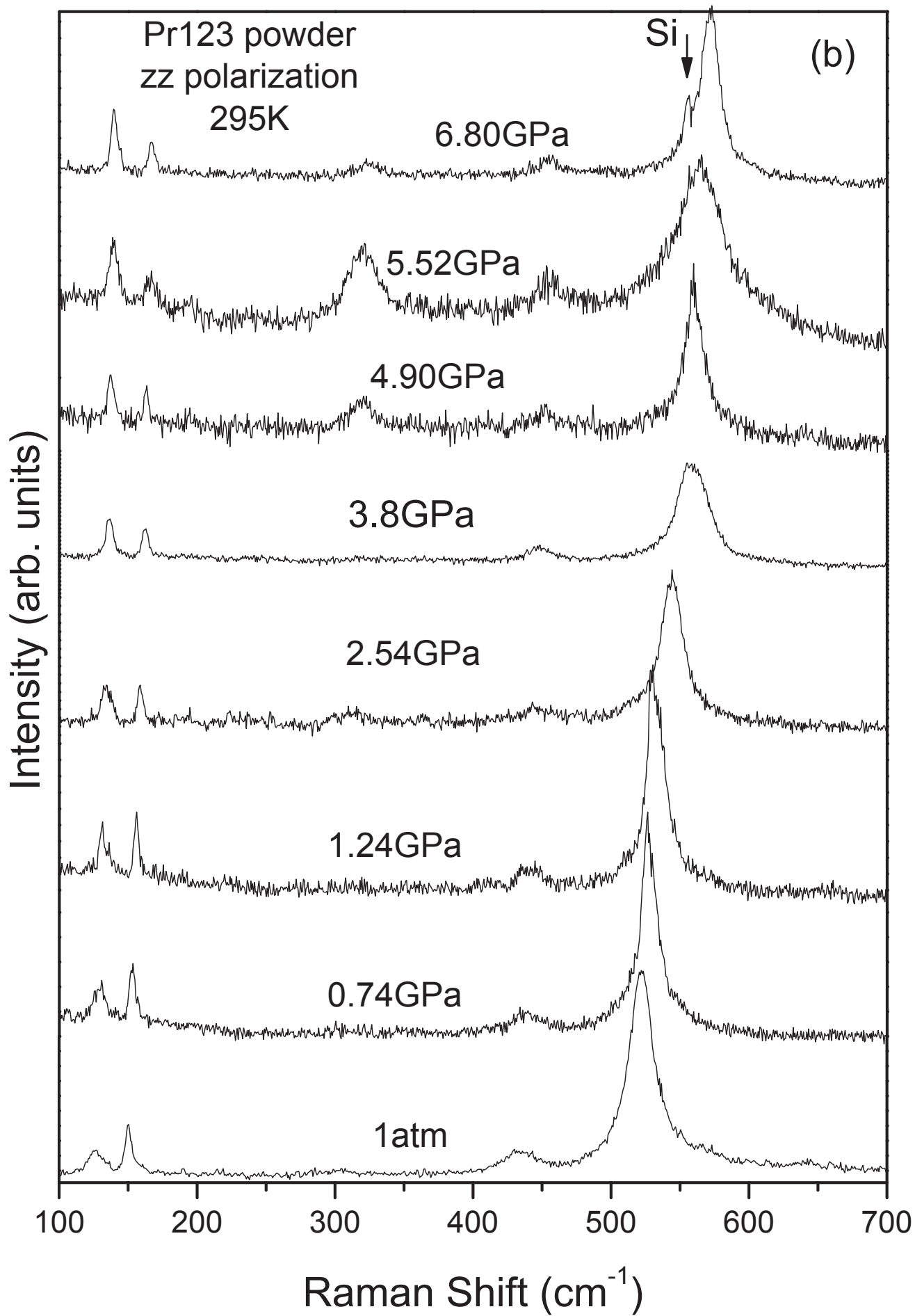
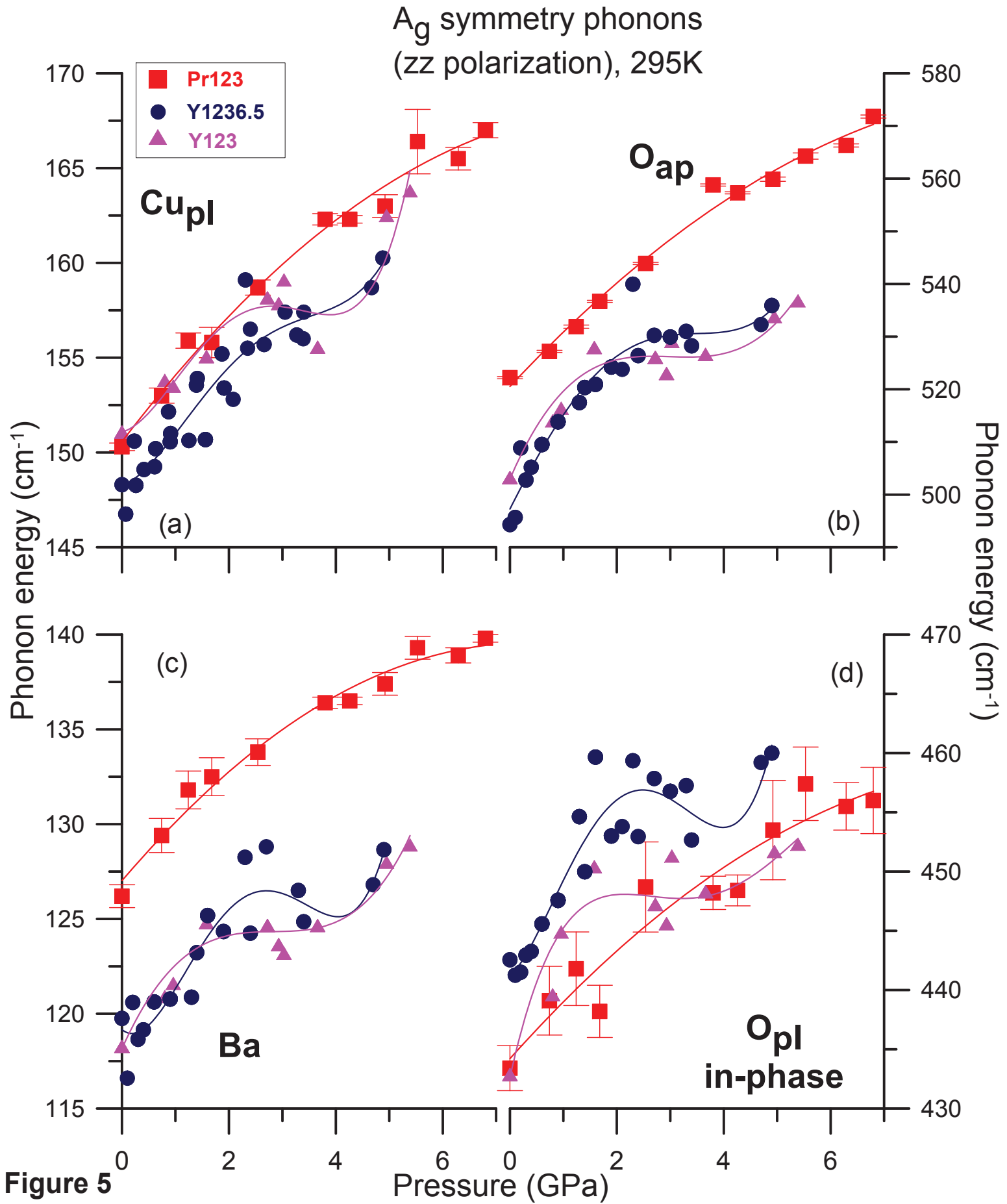
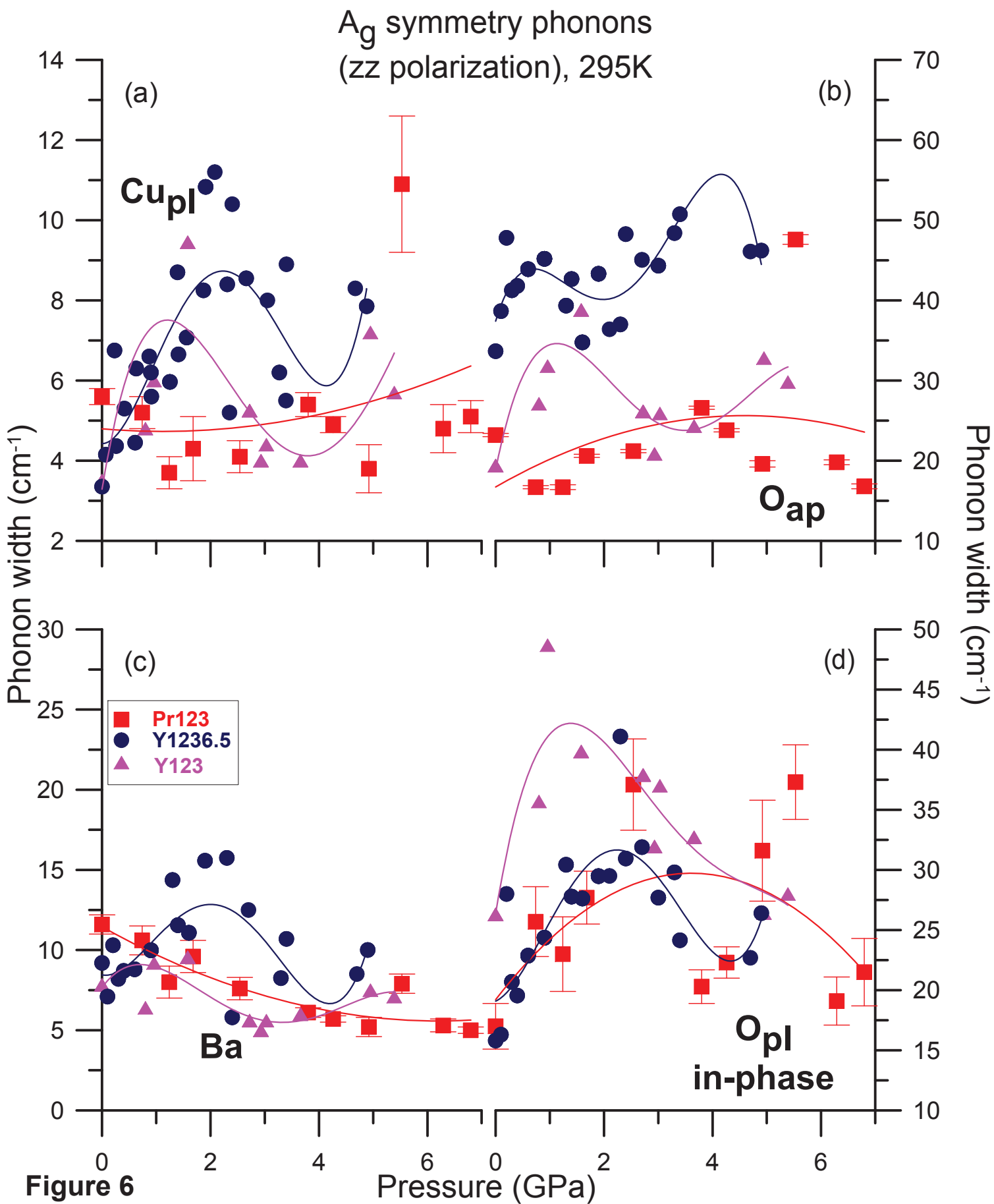


Figure 4b





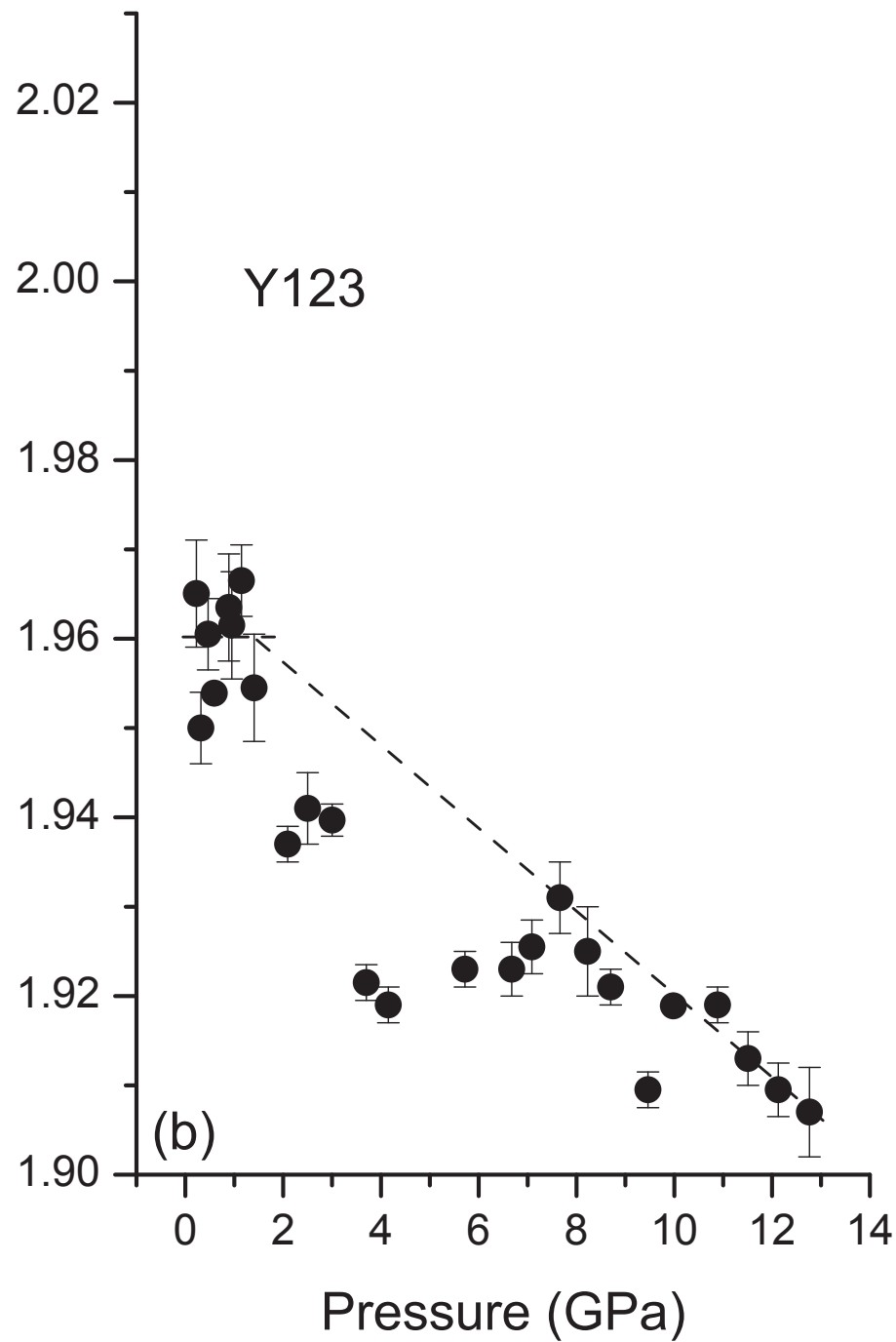
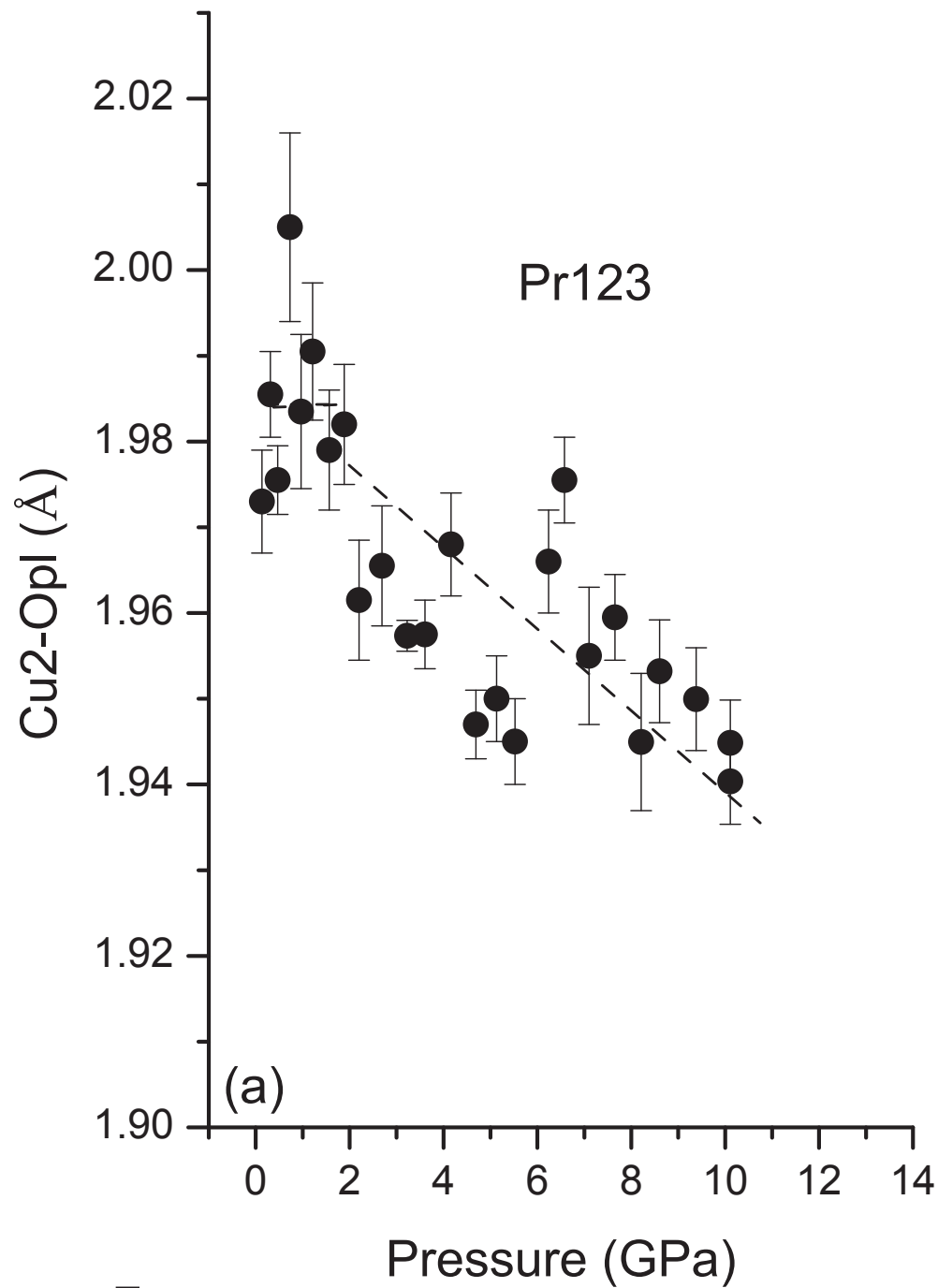


Figure 7